Fast pyrolysis of mannan-rich ivory nut (*Phytelephas aequatorialis*) to valuable biorefinery products

Stef Ghysels, Adriana Elena Estrada Léon, Mehmet Pala, Katharina Alexandra Schoder, Joris Van Acker, Frederik Ronsse

PII: S1385-8947(19)31056-3
DOI: https://doi.org/10.1016/j.cej.2019.05.042
Reference: CEJ 21681

To appear in: *Chemical Engineering Journal*

Revised Date: 6 May 2019
Accepted Date: 8 May 2019

Please cite this article as: S. Ghysels, A.E.E. Léon, M. Pala, K.A. Schoder, J. Van Acker, F. Ronsse, Fast pyrolysis of mannan-rich ivory nut (*Phytelephas aequatorialis*) to valuable biorefinery products, *Chemical Engineering Journal* (2019), doi: https://doi.org/10.1016/j.cej.2019.05.042

Fast pyrolysis of mannan-rich ivory nut (*Phytelephas aequatorialis*) to valuable biorefinery products

Stef Ghysels[a,*], Adriana Elena Estrada Léon[a], Mehmet Pala[a], Katharina Alexandra Schoder[a,b], Joris Van Acker[c], Frederik Ronsse[a]

[a]*Thermochemical Conversion of Biomass Research Group, Department of Green Chemistry and Technology, Ghent University, Coupure Links 653, 9000 Ghent, Belgium.*
[b]*Department of Conversion Technologies of Biobased Resources, University of Hohenheim, Garbenstraβe 9, 70593 Stuttgart, Germany.*
[c]*UGent-Woodlab, Department of Environment, Ghent University, Coupure Links 653, 9000 Ghent, Belgium.*

Abstract

Ivory nut residues from the palm *Phytelephas aequatorialis* were converted *via* fast pyrolysis into a set of valuable biorefinery products, being (i) pyrolysis liquids rich in levomannosan and 5–hydroxymethyl furfural (5–HMF), (ii) biochar, with potential for soil applications, (iii) and non–condensable gases with potential for upgrading and syngas processes. The ivory nut residues were mannan–rich leftovers from button manufacturing in Ecuador. A handful of studies, dating back from the 20th century, have investigated gram–scale valorization of ivory nut to e.g. mannose. Nevertheless, advances in science and technology on biorefinery products called for a comprehensive reassessment of the valorization potential of this underutilized feedstock. A fully equipped, continuously operated lab–scale reactor (200 g.h^{-1} feed) was used for pyrolysis at 350 °C and 500 °C. The pyrolysis liquid yield was 57.53 wt% at 350 °C and 60.36 wt% at 500 °C. The aqueous phase obtained at 350 °C contained 17.5 wt% (d.b.) anhydrosugars, of which 90% was levomannosan, and contained 11.6 wt% (d.b.) furans, of which 56% was 5–HMF and 17% furfural. The carbon stability of the biochars, measured with the Edinburgh accelerated ageing tool, were 40.6 % and 64.6%, respectively. Non-condensable gases during pyrolysis at 350 °C only were composed of CO_2 and CO (CO_2:CO molar ratio of 4:1), while at 500 °C, gases were obtained with a CO_2:CO:H_2:CH_4 molar ratio of 9:9:4:1. Overall, the results demonstrate that pyrolysis of ivory nut holds

*Stef.Ghysels@UGent.be

potential as starting point for valuable biorefinery products.

Keywords: fast pyrolysis, biochar, levomannosan, platform chemicals, biorefinery, ivory nut mannan

1. Introduction

To promote the transition from a fossil-based economy to a bio-based economy, viable and well-thought biorefinery concepts should be put forth. An essential part of this task constitutes the meticulous selection of appropriate conversion and valorization schemes in such way that maximum value is created from the starting material and arising side streams [1, 2, 3].

An ongoing intensification of biorefinery research goes in tandem with research on platform chemicals. These are the building blocks from which commodity, or even new-to-industry, chemicals and materials can be obtained [4]. Lignocellulosic biomass is particularly suited for production of a plethora of platform chemicals. Lignin is increasingly envisaged to substitute petroleum-based benzene, toluene, xylene (BTX) and phenol or to introduce new-to-industry functionalized phenolics [5, 6]. Fig. 1 illustrates that the holocellulose fraction from biomass, *viz.* cellulose and hemicellulose, can typically channel to a more diverse spectrum of products [7, 8].

Each of the chemicals depicted in Fig. 1, like levoglucosan [9], levoglucosenone [10, 11], 5-hydroxymethyl furfural [12, 13, 14], furandicarboxylic acid [15, 16, 17, 18], levulinic acid [19, 20, 21], furfural [22, 23, 24] and γ-valerolactone [25], are of high and specific significance. Levoglucosenone for instance is a well-demonstrated member of the "chiral-pool" [10] and its hydrogenated product, dihydrolevoglucosenone, exerts excellent dipolarity to replace widely used solvents, like e.g. *N*–methylpyrrolidinone (NMP), which is of high-concern due to its toxicity [26]. 5-Hydroxymethyl furfural on the other hand can be deployed within the plastic industry [27], while its derivatives comprise valuable fuel additives [28, 29].

Fermentable sugars from e.g. cellulose are "platform chemicals" themselves; through e.g. biochemical transformations, sugars are converted to molecules like ethanol, itaconic acid, lactic acid, etc.

Fast pyrolysis is a simple conversion technology, able to produce the majority of the aforementioned chemicals from the holocellulose fraction of biomass [30, 31, 32]. The main product from fast pyrolysis is the pyrolysis liquid, which can find applications as a liquid biofuel or from which valuable chemicals can be extracted. Side products from fast pyrolysis are (i) biochar, which can find applications as solid fuel, soil amendment, precursor for activated carbon, etc. and (ii) non-condensable gases, with applications for heat generation or syngas processes. While alternative conversion technologies, like hydrolysis, hydrothermal liquefaction, etc. also can generate liquid biofuels and valuable platform chemicals, fast pyrolysis is particularly attractive, because it can achieve high product yields and has a high throughput [33].

The final application of the main pyrolysis liquids depends upon its properties, but if pyrolysis of biomass is pursued for extracting specific compounds, fractionation of the biomass prior to pyrolysis into lignin, cellulose and hemicellulose typically is required. While this poses a considerable hurdle, it also facilitates simpler downstream processing and purification [34, 35, 36, 37]. To bypass fractionation, particular biomass or waste streams are sought for, which are naturally rich in holocellulose and deficient in lignin, or *vice-versa* [38, 39, 40].

Ivory nut (also called vegetable ivory, tagua or jarina seed) is the white endosperm of the palm species *Phytelephas* [41], grown in the Amazon region and has a pronounced high carbohydrate content and a particularly low lignin and ash content [42, 43]. The carbohydrate within ivory nut is mannan [43, 44, 45, 46, 47, 48]. Timell [43] reported 45% mannan A, 25% mannan B and 7.5% cellulose. Mannan is extracted from ivory nut and is available as CAS 37251-47-1. As a sustainable substitute for ivory [49], vegetable ivory is crafted into buttons, ornaments, etc. and is an inherent part of the local economy of e.g. Ecuador [50] (Fig.2). During the production of buttons from ivory nut, between 65-88% residues are produced, which are the leftovers after cutting small discs out of the ivory nut [42]. With an annual export of 661.7×10^3 kg (Central Bank of Ecuador), the annual production of residues ranges between 1000 and 5000 $\times 10^3$ kg for Ecuador only. For these residues, no proper waste-management strategy exists.

Despite having an advantageous composition for carbohydrate-derived chemicals and coming with a significant quantity, only few studies investigated the valorization (potential) of the

main and side-products in a biorefinery context. These few studies, especially from the 20^{th} century, exclusively investigated pyrolysis for either mannan [43, 44, 45], levomannosan [46, 47] or D-mannose production [51, 52]. Nevertheless, advances in sciences and technology on e.g. carbohydrate-derived platform chemicals accelerated in the very beginning of the 21^{st} century, by which time this ivory nut was virtually out-of-science (Fig. A.1 in Supplementary Information). Moreover, all aforementioned papers investigated ivory nut valorization on gram-scale, while also overlooking the characterization of side-products, like non-condensable gases and biochar.

This work therefore revived pyrolysis research of ivory nut and, for the first time, assessed the potential of pyrolysis products from ivory nut residues towards: (i) liquid biofuels (ii) mannan-derived platform chemicals, (iii) solid biofuels, (iv) soil amendment and (v) syngas processes. Fast pyrolysis was performed using a fully equipped, continuously operated lab-scale reactor. The influence of the pyrolysis reactor temperature on the pyrolysis products, their quantity and quality was assessed and the overall value of a pyrolysis-based biorefinery was evaluated.

2. Materials and Methods

2.1. Ivory nut residues

Ivory nut residues (Fig. 2) were kindly provided by a button manufacturing company, located in the Manabí province, Ecuador. The ivory nut residues were sun-dried for three days in Ecuador before milling (Retsch SM 200 cutting mill). The ivory nut particles were then sieved (Retsch AS 2000) and particles between 1 to 2 mm were retained for pyrolysis experiments. The feedstock composition and its thermal degradation were assessed through micropyrolysis (Py–GC/MS), thermogravimetric analysis coupled to differential scanning calorimetry (TGA-DSC), proximate analysis and elemental analysis. Other analyses on ivory nut were conducted to compare to the solid residue after pyrolysis (*viz.* biochar) and include ash composition analysis, higher heating value determination and Brunauer-Emmett-Teller (BET) surface area analysis (Section 2.4).

To infer the carbohydrate composition of ivory nut and compare it with cellulose, ivory nut and cellulose were subjected to micropyrolysis (i.e. an investigation of their pyrolytic degradation products) by a micropyrolysis unit coupled to a gas chromatograph and mass spectrometer (Thermo Fisher Scientific Trace GC Ultra and Thermo ISQ MS), using a Tandem Pyrolyser RX-3050-TR with HP 3050 Flow Controller from Frontier Laboratories Ltd. The procedure and instrumental details are outlined in Supplementary Information (Section D. The GC/MS part of the micropyrolysis analyses were performed under the same conditions as outlined for GC/MS analysis of the pyrolysis liquids). Briefly, between 300 and 500 μg of ivory nut or and cellulose were weighted and loaded into a sample cup. That sample cup was dropped into a deactivated stainless steel pyrolysis tube, preheated to 350 °C or 500 °C. By doing so, ivory nut and cellulose were very rapidly heated to the pyrolysis temperature (15–20 ms), ensuring rapid pyrolysis with a minimum of side-reactions (like secondary cracking). The pyrolysis vapors were directly swept into the GC using helium as the carrier gas. Component concentrations were expressed in relative abundance (TIC area% is the component peak area divided by the total peak area; TIC represents the total ion count).

TGA-DSC was performed using a Sensys evo TG-DSC thermogravimetric analyzer (SETARAM, France). Approximately 10 mg was subjected to a programmed temperature profile: (i) linear heating 30 °C to 105 °C at 10 °C.min^{-1} (ii) holding at 105 °C for 3 minutes (iii) linear heating from 105 °C to 800 °C at 10 °C.min^{-1}. A constant nitrogen flow ($\geq$ 99.999 % purity, ALPHAGAZ 1, Air Liquide) of 20 mL.min^{-1} was applied.

Proximate analysis was performed, according to Enders and Lehmann [53], which is a refined version of ASTM D1762-84 [54]. Calculations of the moisture, volatile matter, fixed carbon and ash content are detailed in Supplementary Information (Eq. B.1–B.4).

Elemental analysis of the feedstock was performed using a Flash 2000 Elemental Analyzer (Thermo Fisher Scientific, Waltham, MA, USA). Analyses were performed on 2 mg of pre-dried and powdered materials in duplicate. Elements C, H, N and S were measured,

while the oxygen composition was obtained by difference:

$$\mathrm{O\ (wt\%\ d.b.)} = 100\% - \mathrm{C\ (wt\%\ d.b.)} - \mathrm{N\ (wt\%\ d.b.)} - \mathrm{H\ (wt\%\ d.b.)} - \mathrm{S\ (wt\%\ d.b.)} - \mathrm{Ash\ (wt\%\ d.b.)}. \quad (1)$$

As standard reference, 2,5-Bis(5-tert-butyl-benzoxazol-2-yl)thiophene (BBOT) was used.

2.2. Fast pyrolysis

Fast pyrolysis was performed for 30 minutes at two pyrolysis reactor temperatures, both in duplicate. Based on the TGA results (Section 3.1), 350 °C was selected as first pyrolysis reactor temperature. The second was 500 °C, which is a benchmark (standard) temperature for fast pyrolysis.

2.2.1. Experimentation

The experiments were performed in a fully controlled, continuously operated, lab–scale pyrolysis reactor, presented in Fig. 3 (i.e. the set–up described by Yildiz et al. [55] after optimization). The entire set-up was purged with nitrogen gas ($\geq$ 99.8 % purity, industrial, Air Liquide, Belgium) to reach a constant sweep gas rate of 60 $\mathrm{L.h^{-1}}$. The hot vapor residence time was ca. 5 seconds [55]. The biomass conveyor transported ca. 200 g ivory nut per hour to the reactor conveyor, where the feedstock contacted the preheated sand and pyrolysis started. The pyrolysing particles were held long enough into the reactor by automated opening/closing of the pistons and so discarding sand and formed biochar into the collection vessel. By doing so, a solid residence time of ca. 4 minutes was maintained and complete pyrolysis of the biomass was assured. Pyrolysis vapors, swept by nitrogen gas, passed through two knock-out vessels to trap entrained fine solid particles before entering a water-cooled (2 °C) electrostatic precipitator (ESP) and spiral cooler (tap water). Condensable gases were collected as pyrolysis liquids in the two respective liquid collection vessels. Non-condensable gases were finally filtered through a cotton filter and counted by a wet gas meter (Ritter TG 3, Germany). The cumulative volume of evolved gases was recorded and sampled every five minutes for composition analysis by GC.

2.2.2. Mass and carbon balance closure

The mass balance closure or overall yield $Y_{\mathrm{m,overall}}$ was obtained by summing up the yields of pyrolysis liquids (PL), biochar (BC) and non-condensable gases (NCG) relative to the feedstock mass:

$$Y_{\mathrm{overall}} = Y_{\mathrm{PL}} + Y_{\mathrm{BC}} + Y_{\mathrm{NCG}}. \quad (2)$$

Detailed calculation of the yield in Eq. 2 is provided in Supplementary Information (Eq. C.1-C.2). The carbon balance closure or overall carbon yield $Y_{\mathrm{C,overall}}$ was obtained by multiplying the mass of all pyrolysis products (aqueous phase, $\mathrm{PL_{ap}}$, and organic phase, $\mathrm{PL_{op}}$) and feedstock by their respective carbon contents ($\mathrm{g.g^{-1}}$):

$$Y_{\mathrm{C,overall}} = \frac{m_{\mathrm{BC}} \times C_{\mathrm{BC}} + m_{\mathrm{PL_{aq}}} \times C_{\mathrm{PL_{aq}}} + m_{\mathrm{PL_{op}}} \times C_{\mathrm{PL_{oil}}} + m_{\mathrm{NCG}} \times C_{\mathrm{NCG}}}{m_{\mathrm{FS}} \times C_{\mathrm{FS}}}. \quad (3)$$

The carbon content of the feedstock, biochar and pyrolysis liquids (both phases) were obtained through elemental analysis (Section 2.1), while the carbon content of the non-condensable gases was calculated from their composition.

2.3. Pyrolysis liquids characterization

Compositional analysis and quantification of the detected compounds within the phase-separated pyrolysis liquids were performed through GC–MS analysis (Thermo Fisher Scientific Trace GC Ultra and Thermo ISQ MS). Between 0.20-0.25 g of the pyrolysis liquid (either aqueous, either organic phase) was mixed with 100 μL of a 2.5 wt% fluoranthene (98%, Sigma Aldrich) solution in acetonitrile ($\geq$99.5%, Carl Roth) as internal standard and diluted with 5 g acetonitrile. This solution with ca. 5 wt% analyte was injected (injector temperature of 250 °C, split ratio of 1:100) and separated on a RTX-1701 chromatographic column (Restek, 60 m $\times$ 0.25 mm, 0.25 μm). A detailed description of instrumental parameters is provided in Supplementary Information (Section E.1).

The GC–MS was calibrated with a set of reference compounds typically found in pyrolysis liquids, which were directly quantified. Detected chemical compounds for which the GC–MS was not calibrated were quantified by using the response factors from calibrated compounds with structural similarity or which belong to the same chemical group [56]. Table E.1 in

Supplementary Information provides an overview of the calibrated reference compounds and indicates which response factors were used to quantify the reported chemical compounds. The water content of the aqueous phase and organic phase of the pyrolysis liquids was determined by Karl Fischer titration (Mettler Toledo V20; 5 ml burette; electrode: DM 143-SC; reagent: Merck Titrant 5 Keto; solvent: Merck combi Solvent 5 Keto). Triplicate measurements were performed on each pyrolysis liquid phase, except on the organic phase from the experiments performed at 350 °C. There was too little organic phase to analyze; its water content was assumed equal to that of the organic phase at 500 °C. The obtained amount of pyrolytic water (i.e. chemical water from the pyrolysis reaction), relative to the dry biomass input, was calculated by subtracting the amount of feedstock water from the total amount of obtained water found in the pyrolysis liquids.

The calorific values of the aqueous phase, organic phase and the total pyrolysis liquids were calculated from the relation reported by Channiwala and Parikh [57]:

$$\mathrm{HHV_{dry}} = 0.349\mathrm{C} + 1.1738\mathrm{H} + 0.1005\mathrm{S} - 0.1034\mathrm{O} - 0.151\mathrm{N} - 0.0211\mathrm{A}. \qquad (4)$$

$\mathrm{HHV_{dry}}$ $(\mathrm{MJ.kg^{-1}})$ represents the calorific value of the specific pyrolysis liquid phase on dry basis, while the C, H, O, N, S and A represents carbon, hydrogen, oxygen, nitrogen, sulphur and ash contents of the material, respectively, expressed in mass percentages on dry basis. The ash content of the bio-oils was assumed zero. The calorific value of the as-produced $\mathrm{HHV_{a.p.}}$, $(\mathrm{MJ.kg^{-1}})$ pyrolysis liquid (phases) was obtained by taking into account their water content [58]:

$$\mathrm{HHV_{a.p.}} = \mathrm{HHV_{dry}} \times \frac{100 - \mathrm{water\ content_{pyrolysis\ liq.}(wt\%)}}{100}. \qquad (5)$$

Elemental analyses of the two pyrolysis liquid phases was performed as described in Section 2.1, using 2-2.5 mg of each phase. The elemental composition of the pyrolysis liquid phases on a dry basis (d.b.) were calculated, based on the water content of the pyrolysis liquid phases.

2.4. Biochar characterization

Ash compositional analysis, higher heating value determination, carbon stability tests and Brunauer-Emmett-Teller (BET) surface area analysis were performed on the biochars, in

addition to proximate analysis and elemental analysis.

To perform ash compositional analysis, biochar (and as well as ivory nut) were first ashed under the same conditions as for proximate analysis (Section 2.1). 100 mg of the ash was dissolved in 5 vol% HNO_3 (Chem-Lab, Zedelgem, Belgium) to a volume of 25 ml for analysis by Inductively Coupled Plasma - Optical Emission Spectroscopy (ICP–OES, Varian MPX, Palo–Alto, CA). To quantify the ash constituents, a calibration set was prepared (0-100 mg/l) and accepted if $R^2 > 0.995$. The following expected elements in biomass and biochar [59] were quantified with their respective wave length: Ca, 396.85 nm; Mg, 280.27 nm; K, 766.49 nm; Na, 589.59 nm; Cr, 267.72 nm; Mn, 257.61 nm; Fe, 238.20 nm; Co, 238.89 nm; Ni, 231.60 nm; Cu, 327.39 nm; Zn, 213.86 nm. The ash recovery was calculated as follows:

$$\text{Ash recovery} = \frac{\text{Ash}_{\text{BC}} \times Y_{\text{BC}}}{\text{Ash}_{\text{FS}}}, \tag{6}$$

where Ash_{BC} and Ash_{FS} represent the ash contents of the biochar and biomass (as calculated in Supplementary Information, Eq. B3) and Y_{BC} represents the biochar yield. The element recovery is similarly obtained by replacing the ash contents in Eq. 6 with the individual element content.

The higher heating value (HHV) of the biochar and feedstock were determined using an e2k combustion calorimeter (Digital Data Systems (PTY)) in duplicate. The HHV of benzoic acid (IKA, C 723) was analysed and compared with the manufacturer's reference (26.454 MJ.kg^{-1}) to assess the accuracy of the device prior to the tests. The subjected biochars and feedstock were pre-dried at 105 °C, of which a pre-weighted amount (ca. 0.4 g) was introduced in a pre-weighted gelatin capsule (ca. 0.09 g). The bomb was pressurized to 3000 kPa with pure oxygen ($\geq$ 99.995 % purity, ALPHAGAZ 1, Air liquide, Belgium). The HHV of the sample ($\text{HHV}_{\text{sample}}$) was obtained from Eq. 7:

$$\text{HHV}_{\text{total}} = \text{wt}\%_{\text{capsule}} \times \text{HHV}_{\text{capsule}} + \text{wt}\%_{\text{sample}} \times \text{HHV}_{\text{sample}}, \tag{7}$$

where $\text{HHV}_{\text{total}}$ represents the reading from the e2k combustion calorimeter.

Carbon stability of the produced biochars was determined in triplicate according to the Edinburgh stability tool, which induces the artificial oxidative aging of the biochar [60]

(details in Supplementary Information, Section F). The biochar carbon stability (%) was calculated as:

$$\text{Carbon Stability (\%)} = \frac{\mathrm{BC_{r,ox}} \times \mathrm{C_{BC_{r,ox}}}}{\mathrm{BC_i} \times \mathrm{C_{BC_i}}}, \tag{8}$$

where $\mathrm{BC_{r,ox}}$ represents the residual mass of the biochar after oxidation and $\mathrm{BC_i}$ the initial mass of the tested biochar. $\mathrm{C_{BC_{r,ox}}}$ and $\mathrm{C_{BC_i}}$ represent their respective carbon contents (wt%), as determined through elemental analysis.

2.5. Non-condensable gases characterization

The non-condensable gases were sampled during pyrolysis every five minutes and subsequently analyzed in a micro GC (Varian Micro-GC 490-GC) with two analytical columns: 10 m Molesieve 5A (with backflush) and 10 m PPQ with thermal conductivity detectors (TCD), using helium and argon as carrier gases. The first column separated and quantified (vol%) H_2, O_2, N_2, CH_4 and CO (in order of occurrence of the peaks), whereas CO_2, C_2H_4, C_2H_6 and C_3H_6/C_3H_8 were separated and quantified (vol%) in the second column.

3. Results and Discussion

3.1. Ivory nut residues

Results of the micropyrolysis experiments in Table 1 show that more than half (53.00%) of the TIC–area is levomannosan, which is the pyrolysis product from mannan. The TIC-area% of levoglucosan obtained from cellulose was 75.25%. As the anhydrosugar levomannan constituted the largest TIC area% upon micropyolysis of ivory nut (like levoglucosan from cellulose), the mannan-rich nature of ivory nut described in literature is supported. Next to levomannosan, fast pyrolysis of ivory nut also led to appreciable TIC area% of 5–hydroxymethyl furfural (5–HMF).

The TGA and dTGA in Fig. 4a show a narrow range of fast volatilization between 250 °C to 350 °C. At temperatures exceeding 350 °C, mass-loss leveled. Therefore, 350 °C was chosen as one of the pyrolysis reactor temperatures for this study. The highest mass-loss rate occurred at 300 °C, which is close to (i.e. slightly higher) that of hemicellulose, approximated by xylan, but smaller than expected for cellulose (350 °C) [61, 62]. The residual mass at

approximately 800 °C was ca. 26% and also is in line with typical values found for hemicellulose [61]. The presented TGA in Fig. 4a aligns well with that observed by Furneaux and Shafizadeh [46]. The exothermal peak in differential scanning calorimetry (Fig. 4b) at 300 °C aligns neatly with the peak of steepest mass-loss in dTGA. These results suggests a hemicellulose-like composition, as hemicellulose also shows a similar peak [61] and further confirms mannan as hemicellulose constituent in ivory nut.

The moisture content was 12.41 ± 0.03 wt%, the volatile matter content 82.39 ± 0.05 wt% d.b., the ash content 0.95 ± 0.0 wt% d.b. and the fixed carbon content 16.67 ± 0.07 wt% d.b. The volatile matter content was significantly higher (10%) than the volatile matter typically reported for lignocellulosic biomass. This is due to the high carbohydrate fraction in ivory nut and is related to the high mass-loss observed during the TGA. This property is advantageous from a pyrolysis point-of-view. A high volatile matter content results in a high yield of pyrolysis liquids (condensable vapors), which contain the mannan-derived pyrolysis products of interest. The measured ash content was considerably low, compared to other agricultural residues like grass and straw (which can have up to 10 wt% d.b.), and falls within the range of those previously reported: 1.08% - 1.60% [46, 63, 42]. This is also considered advantageous for pyrolysis liquid yields: the less alkali metals (found in the ash), the less extensive secondary cracking of the valuable carbohydrate-derived compounds (like anhydrosugars and 5-hydroxymethyl furfural) to light oxygenates and non-condensable gases [64, 65, 66].

From the elemental analysis (C: 44.89 ± 0.35 wt% d.b.; H: 6.69 ± 0.04 wt% d.b.; N: 0.38 ± 0.04 wt% d.b.; O: 47.10 ± 0.28 wt% d.b.), the elemental composition was: $C_6H_{11}O_5N_{0.3}$, which reflects the carbohydrate-rich nature. Nitrogen, probably in a protein–bound form, was also present within ivory nut. A picture is provided in Supplementary Information (Figure H.2), which shows a significant browning after spending one week at 105 °C. The browning was attributed to Maillard reactions between the protein and carbohydrate fractions within ivory nut.

Overall, the properties indicate that ivory nut residues hold potential towards fast pyrolysis for pyrolysis liquids production (with mannan-derived platform chemicals). The feedstock

is carbohydrate-rich (TGA, elemental analysis), with little ash (proximate) and a high tendency for volatilization (TGA, proximate).

3.2. Fast pyrolysis

3.2.1. Experimentation

Ivory nut appeared a good substrate for pyrolysis in a fully-equipped auger pyrolysis reactor. Its feeding in the biomass conveyor was particularly consistent (198.45 ± 2.88 g/h), due to its non-fibrous and hard nature. The ivory nut did not melt or froth during pyrolysis, as was also stated by Furneaux and Shafizadeh [46].

3.2.2. Mass- and carbon balance closure

The mass balance closures are presented in Fig. 5a and are near 100%. The product with the highest yield after fast pyrolysis was the pyrolysis liquid, both at a pyrolysis reactor temperature of 350 °C and 500 °C. During condensation of the condensable pyrolysis vapors in the ESP, spontaneous phase separation occurred into an aqueous phase and an organic phase. The aqueous phase accounted for 96 ± 1 % of the pyrolysis liquids produced at 350 °C, while the pyrolysis liquids obtained at 500 °C comprised 86 ± 1 % of aqueous phase. Pyrolysis of ivory nut reached similar liquid yields as previously reported for pine wood at 500 °C in a similar set-up [55], but were smaller than those reported for e.g. fluidized bed pyrolysis reactors (65-75 wt%) [62], due to the difference in hot vapour residence time. The mass balances in Fig. 5a show an increasing yield in non-condensable gases and decreasing yield in biochar upon an increase of in pyrolysis reactor temperature from 350 °C to 500 °C, while the pyrolysis liquid yield remained similar. The produced biochar at 350 °C had an apparent odor, which indicated that some volatile compounds were retained on the solid phase (see Section 2.4). During pyrolysis at 500 °C, volatile compounds partitioned virtually entirely to the condensable gas fraction, but also underwent secondary cracking more extensively. This led to the apparent equal yield in pyrolysis liquids.

The carbon balance in Fig. 5b illustrates the distribution of carbon among the pyrolysis products. For the pyrolysis products obtained at 350 °C, most of the carbon is found in the biochar. The aqueous phase of the pyrolysis liquid obtained at 350 °C had less carbon:

ca. 28 wt%. Upon an increase of the pyrolysis reactor temperature, the carbon distributed more equally over the pyrolysis products. Although the organic phase from pyrolysis at 500 °C is 14 wt% of the pyrolysis liquids, it contributes to 43.5 wt% of the carbon content of all liquids phases. This is also reflected in the HHV of the organic phase of liquids from 500 °C pyrolysis, being 28.19 $MJ.kg^{-1}$ (d.b.), which is higher than the HHV of the corresponding aqueous phase (22.55 $MJ.kg^{-1}$). For biofuel purposes, high carbon yields and calorific values are pursued for the pyrolysis liquids. For non-fuel applications of specific compounds within the liquids, like anhydrosugars, 5-hydroxymethyl furfural, a more complete analysis of the pyrolysis liquids is required as these chemicals have considerable oxygen quantities as well.

3.3. Pyrolysis liquids composition and relevance

Table 2 presents the elemental composition of both pyrolysis liquid phases, obtained at 350 °C and 500 °C. The results are shown on an "as-produced" (a.p.) basis (wt%) and on a dry basis (d.b.). The water content, which was used to calculate the elemental composition on dry basis, is also presented in Table 2. The results show that the aqueous phase holds ca. 60 wt% of water, while the organic phase contains ca. 12 wt% water, regardless of the pyrolysis reactor temperature. The yield in pyrolytic water, expressed on a dry biomass basis, was ca. 23 wt% for both pyrolysis temperatures, meaning that 100 g of dry biomass would yield ca. 23 g pyrolytic water.

On an as-produced basis, the organic phase from both pyrolysis temperatures was rich in carbon and poor in oxygen, compared to the corresponding aqueous phases. If expressed on a dry basis, the elemental compositions of the aqueous phase approached that of the organic phase, but still with significant difference in the carbon content. The atomic O/C and H/C ratio of the *aqueous* phase from 350 °C (O/C: 0.62 and H/C: 1.88) and 500 °C (O/C: 0.61 and H/C: 2.04) were relatively similar. In contrast, the *organic* phase of the pyrolysis liquids from both temperatures changed in elemental composition: the carbon content increased, while the oxygen content decreased (O/C: 0.50 at 350 °C to O/C: 0.37 at 500 °C). The most abundant compound according to GC–MS analysis (*vide infra* and

Supplementary Information, Table I.2) in the organic phase obtained at 350 °C was 5-hydroxymethyl furfural, for which the O/C and H/C ratios are O/C: 0.5 and H/C: 1 and in line with that of the organic phase (O/C: 0.50 and H/C: 1.13). The same holds for the O/C and H/C ratios of the heavy oil phase at 500 °C (O/C: 0.37 and H/C: 1.20) and its most abundant compound (i.e. 5-methylfurfural, O/C: 0.33 and H/C: 1). This indicates that the quantity of high-molecular weight compounds, typically (aromatic) repolymerization products (not detectable through GC–MS), can be considered moderate.

Results of the GC–MS analysis are summarized in Fig. 5c and 5d. Compound-specific concentrations can be found in Fig. 6 and Supplementary Information (Table I.2). The aqueous phase obtained at 350 °C had a pronounced high concentration of anhydrosugars (17.5 wt% d.b.). The main constituent of the anhydrosugars was levomannosan (90% of the mass fraction of anhydrosugars in the pyrolysis, Table E.1 and I.2 in Supplementary Information), which is the mannan analogue to levoglucosan from cellulose. The class furans also reached high quantities in the aqueous phase (11.6 wt% d.b., Fig. 5c). 5–HMF and furfural represented 56% and 17% respectively of the mass fraction of furans in the pyrolysis liquids. An increase of the pyrolysis reactor temperature from 350 °C to 500 °C caused an increase in light oxygenates, like carboxylic acid (acetic acid), aldehydes (hydroxyacetaldehyde) and ketones (acetol), at the expense of anhydrosugars and furans. The total quantity of phenolic compounds was very limited in both phases, due to the low fraction of lignin in this biomass. The organic phase, from both pyrolysis reactor temperatures, was rich in furans (Fig. 5d). Upon pyrolysis at 350 °C, 5-HMF was the most abundant furan (representing 49% of the total furan concentration), while furfural was the most abundant furan within the organic phase obtained from pyrolysis at 500 °C. An increase of the pyrolysis reactor temperature also caused a decrease in furans and anhydrosugars in the organic phase, but less extensive as for the aqueous phase.

The composition of the obtained pyrolysis liquids is unique and reflects the unique composition of ivory nut. While lignocellulosic biomass results in high concentrations of carboxylic acids and phenolics [56], fewer quantities of these were found in neither the aqueous phase, nor the organic phase. The pyrolysis liquids also combined typical characteristics expected for liquids obtained from hemicelluloses (i.e. high acetol concentration) and cellulose (i.e. high

concentration of anhydrosugars) [67, 68]. A special feature however is the high ratio of furans over anhydrosugars in the aqueous phase (0.67 at 350 °C, 0.87 at 500 °C) and organic phase (4.97 at 350 °C, 11.2 at 500 °C), which is not observed for pure cellulose in either micropyrolysis experiments, or in a fluidized bed reactor of similar scale (100 $g.h^{-1}$ feeding) [67]. There is thus a natural tendency of ivory nut towards furfural compounds, especially 5-hydroxymethyl furfural, methylfurfural and furfural, which was also apparent from micropyrolysis analysis of ivory nut in Table 1. This is also in line with Hu et al. [30], who stated that mannose during pyrolysis results in more 5–HMF that glucose does, due to the epimerization of the C2 position. Fig. 6 provides a possible reaction scheme of mannan (major compound) and cellulose (minor compound) during fast pyrolysis. The yield in the compounds is an indication within each phase for both pyrolysis reactor temperatures.

Overall, pyrolysis of vegetable ivory directly resulted in pyrolysis liquids, with a specific set of carbohydrate-derived platform chemicals, from which 5-hydroxymethyl furfural is most noteworthy. Levomannosan on the other hand has limited direct application, but can be extracted for consecutive dehydration towards levoglucosenone or for the production of mannose. While both levoglucosenone and mannose find multiple applications in chemistry [69, 70], they might increase 5-HMF throughput as well *via* catalytic dehydration [71] and isomerization [72]. Further conversion routes from 5-HMF are depicted in Fig. 1. In fact, a large portion of platform chemicals illustrated in Fig. 1 were found in the pyrolysis liquids or can lead to them.

3.4. Biochar application-relevant properties

Assessing the valorization potential of evolved side products, *viz.* biochar and NCGs, is also important for a biorefinery approach (Introduction). Table 3 presents the obtained results from proximate and elemental analysis. After pyrolysis at 350 °C, biochar was obtained at 33 wt%. However, its volatile matter content (41.6 wt% d.b.) was still significant, which explained the odor of that biochar (Section 3.2.2). The volatile matter content for biochars obtained upon pyrolysis at 500 °C was approximately half the value of that for biochars obtained at 350 °C. On the other hand, the fixed carbon content of the obtained biochar

samples increased from 53.40% to 68.56%, upon increasing the pyrolysis reactor temperature. This was within expectations as the H/C and O/C molar ratios decreased in tandem (Table 3). Nevertheless, variations of the fixed carbon yield are not commonly observed. Instead, the decreasing biochar yield is often balanced with an accompanied increase of the remaining biochar's fixed carbon content, if the pyrolysis reactor temperature increases [73]. In this case, the extensive drop in the biochar yield from 33.00% (350 °C) to 14.34% (500 °C) caused the fixed carbon yield to drop by approximately 50%.

The ash fraction within the biochar was well-retained from the parent feedstock: the ash recoveries for biochar produced at 350 °C and 500 °C were 128% and 129%, respectively. Measured quantities of alkali metals and other nutrients are reported in Table 4. A general observation, along with the ash recovery, is that individual elements were well-retained within the solid phase. The recovery of individual elements in biochar obtained at 500 °C had a weighted average of 121% and was in line with the overall ash recovery. The element recovery for biochar obtained at 350 °C was however significantly above 100%.

Upon soil amendment of biochar, the biorefinery concept becomes carbon-negative, as biochar is more recalcitrant than the original biomass, and so mineralizes to CO_2 slower than the uptake of CO_2 by biomass [74]. Table 3 presents the results from carbon stability tests with hydrogen peroxide. After pyrolysis at 350 °C, a carbon stability of 40.6% was obtained, which increased to 64.6% if pyrolysed at 500 °C. Suchlike increase of the carbon stability in tandem with the pyrolysis reactor temperature is commonly observed and aligns with the results observed by Cross and Sohi [60] for biochar from sugarcane bagasse after *slow* pyrolysis. At 350 °C the average carbon stability of biochar from sugarcane bagasse was on average 44.4%, while at 450 °C, the carbon stability was 69.2%. This indicates that the obtained biochars show approximately an equal fraction of stable carbon, compared to slow pyrolysis biochar, which might also favor soil applications.

Alternatively to soil applications, the biochar can be used to recover heat upon incineration. Indeed, both biochars show elevated higher heating values, compared to the original feedstock. Also, the small increase of the HHV with the pyrolysis reactor temperature was significant, according to a paired t-test with $\alpha = 0.05$.

3.5. Non-condensable gases composition

The molar composition of the non-condensable gases for the different pyrolysis experiments is illustrated in Fig. 7. Note that Fig. 7 represents the nitrogen-free fraction only. The amount of nitrogen within the tail-gases depends on the reactor configuration. During pyrolysis at 350 °C, the formed non-condensable fraction mainly constitutes carbon dioxide and carbon monoxide. This indicates decarboxylation and decarbonylation reactions during pyrolysis at moderate temperature. If pyrolysis was performed at 500 °C, a more diverse set of gases was detected. Carbon dioxide decreased, while carbon monoxide and hydrogen gas increased dramatically. Also, methane and other light hydrocarbons were detected, which will add calorific value to these off-gases.

Next to energy recovery systems, these off-gases can also be considered for chemicals/ fuels production by means of e.g. syngas fermentation or Fischer-Tropsch synthesis. The present H_2/CO ratio of gases evolved during pyrolysis at 500 °C is approximately 0.5, while an ideal ratio for Fischer-Tropsch is 2 or even 3, depending on the envisaged end-product. For syngas fermentation, this ratio is less restrictive. Nevertheless, the contribution of hydrogen gas can be increased through e.g. performing the water-gas shift reaction. Alternatively, fermentation can also be performed with carbon dioxide and hydrogen gas to bioplastics [75]. In such case, all carbon monoxide can be converted to hydrogen gas through the water-gas shift reaction.

3.6. Relevance of this work and future perspectives

In this work, the residues of ivory nut from a button factory were converted *via* pyrolysis into pyrolysis liquids, biochar and non-condensable gases. The pyrolysis liquids were water-rich, which is a disadvantage for biofuel applications, but contained an attractive set of platform chemicals (Fig. 6). Although there is room for optimization, this study already demonstrates a potential of ivory nut towards platform chemicals, like e.g. 5-HMF and others, during pyrolysis. The low non-carbohydrate content of ivory nut can avoid fractionation and may therefore facilitate extraction of the pyrolysis liquids in subsequent steps. The biochar on the other hand holds potential for carbon sequestration, while the non-condensable gases

can be upgraded and used for syngas processes.

The interplay of pyrolysis temperature and product quantity/ composition already allows some tailoring of the process. Indeed, the pyrolysis liquids obtained at 350 °C were valuable in terms of composition, while the non-condensable gases and biochar were better in quality after pyrolysis at 500 °C. However, future research might investigate other opportunities, like catalysis within pyrolysis, to increase the yield of specific compounds with added-value, like e.g. 5–HMF [76].

The ivory nut residues are agricultural waste, which lacked proper valorization. This work demonstrates the potential for pyrolysis to install a meaningful valorization scheme to suchlike inevitable waste (i.e. existing waste that makes part of a local economy).

4. Conclusions

This work investigated fast pyrolysis of ivory nut in a continuous process, the feedstock's properties and the quantity/ quality of evolved pyrolysis products. The mannan-rich ivory nut residues showed features which are favorable for fast pyrolysis at large scale, like (i) the feedstock's thermal degradation pattern with a steep mass-loss rate at 300 °C, (ii) the high volatile matter (approx. 80 wt%) and (iii) low ash content (<1 wt%). The main product, i.e. pyrolysis liquids, was obtained at an average yield of ca. 60 wt% and was rich in levomannosan and 5–hydroxymethyl furfural. Valuable side products (i.e. biochar and non-condensable gases) were also obtained. Biochar had a high ash recovery and could be used for soil amendment and for carbon sequestration. Non-condensable gases obtained during pyrolysis at 500 °C could be used for heat recovery and might offer opportunities for syngas processes upon its upgrading.

Acknowledgements

Dr. ir. Karel Folens from the Laboratory of Analytical Chemistry and Applied Ecochemistry (Ecochem) for ash compositional analysis (Ghent University), Funda Aliç from the department of inorganic and physical chemistry, center for ordered Materials, organometallics & Catalysis

(COMOC) (Ghent University) for BET analysis, Simon Backx from the Synthesis, Bioresources and Bioorganic Chemistry Research Group (SynBioC) (Ghent University) for the fruitful discussions on carbohydrate chemistry.

Statements

The authors declare no competing interests. This research did not receive any specific grant from funding agencies in the public, commercial, or not-for-profit sectors.

Appendix A. Supplementary information

Supplementary information associated with this article can be found, in the online version, at doi.

References

[1] T. J. Farmer, M. Mascal, Platform Molecules, chap. 4, Wiley-Blackwell, ISBN 9781118714478, 89–155, doi:\bibinfo{doi}{10.1002/9781118714478.ch4}, 2014.

[2] L. Filiciotto, A. M. Balu, J. C. V. der Waal, R. Luque, Catalytic insights into the production of biomass-derived side products methyl levulinate, furfural and humins, Catal. Today 302 (2018) 2 – 15, ISSN 0920-5861, doi:\bibinfo{doi}{https://doi.org/10.1016/j.cattod.2017.03.008}.

[3] A. A. Koutinas, A. Vlysidis, D. Pleissner, N. Kopsahelis, I. Lopez Garcia, I. K. Kookos, S. Papanikolaou, T. H. Kwan, C. S. K. Lin, Valorization of industrial waste and by-product streams via fermentation for the production of chemicals and biopolymers, Chem. Soc. Rev. 43 (2014) 2587–2627, doi:\bibinfo{doi}{10.1039/C3CS60293A}.

[4] J.-V. Bomtempo, F. Chaves Alves, F. de Almeida Oroski, Developing new platform chemicals: what is required for a new bio-based molecule to become a

platform chemical in the bioeconomy?, Faraday Discuss. 202 (2017) 213–225, doi:\bibinfo{doi}{10.1039/C7FD00052A}.

[5] M. Windt, D. Meier, J. H. Marsman, H. J. Heeres, S. de Koning, Micro-pyrolysis of technical lignins in a new modular rig and product analysis by GCMS/FID and GCGCTOFMS/FID, J. Anal. Appl. Pyrolysis 85 (1) (2009) 38 – 46, ISSN 0165-2370, doi:\bibinfo{doi}{https://doi.org/10.1016/j.jaap.2008.11.011}, pyrolysis 2008.

[6] S. Van den Bosch, W. Schutyser, R. Vanholme, T. Driessen, S.-F. Koelewijn, T. Renders, B. De Meester, W. J. J. Huijgen, W. Dehaen, C. M. Courtin, B. Lagrain, W. Boerjan, B. F. Sels, Reductive lignocellulose fractionation into soluble lignin-derived phenolic monomers and dimers and processable carbohydrate pulps, Energy Environ. Sci. 8 (2015) 1748–1763, doi:\bibinfo{doi}{10.1039/C5EE00204D}.

[7] S. Takkellapati, T. Li, M. A. Gonzalez, An overview of biorefinery-derived platform chemicals from a cellulose and hemicellulose biorefinery, Clean Technol. and Environ. Policy 20 (7) (2018) 1615–1630, ISSN 1618-9558, doi:\bibinfo{doi}{10.1007/s10098-018-1568-5}.

[8] H. Kobayashi, A. Fukuoka, Synthesis and utilisation of sugar compounds derived from lignocellulosic biomass, Green Chem. 15 (2013) 1740–1763, doi:\bibinfo{doi}{10.1039/C3GC00060E}.

[9] X. Hu, L. Wu, Y. Wang, D. Mourant, C. Lievens, R. Gunawan, C.-Z. Li, Mediating acid-catalyzed conversion of levoglucosan into platform chemicals with various solvents, Green Chem. 14 (2012) 3087–3098, doi:\bibinfo{doi}{10.1039/C2GC35961H}.

[10] M. B. Comba, Y.-h. Tsai, A. M. Sarotti, M. I. Mangione, A. G. Surez, R. A. Spanevello, Levoglucosenone and Its New Applications: Valorization of Cellulose

Residues, Eur. J. Org. Chem. 2018 (5) (2017) 590–604, doi:\bibinfo{doi}{10.1002/ejoc.201701227}.

[11] A. R. S. Teixeira, A. L. Flourat, A. A. M. Peru, F. Brunissen, F. Allais, Lipase-Catalyzed Baeyer-Villiger Oxidation of Cellulose-Derived Levoglucosenone into (S)-γ-Hydroxymethyl-α,β-Butenolide: Optimization by Response Surface Methodology, Front. Chem. 4 (2016) 16, ISSN 2296-2646, doi:\bibinfo{doi}{10.3389/fchem.2016.00016}.

[12] Z. Yuan, C. C. Xu, S. Cheng, M. Leitch, Catalytic conversion of glucose to 5-hydroxymethyl furfural using inexpensive co-catalysts and solvents, Carbohydr. Res. 346 (13) (2011) 2019 – 2023, ISSN 0008-6215, doi:\bibinfo{doi}{https://doi.org/10.1016/j.carres.2011.06.007}.

[13] D. Gupta, E. Ahmad, K. K. Pant, B. Saha, Efficient utilization of potash alum as a green catalyst for production of furfural, 5-hydroxymethylfurfural and levulinic acid from mono-sugars, RSC Adv. 7 (2017) 41973–41979, doi:\bibinfo{doi}{10.1039/C7RA07147G}.

[14] A. Chinnappan, C. Baskar, H. Kim, Biomass into chemicals: green chemical conversion of carbohydrates into 5-hydroxymethylfurfural in ionic liquids, RSC Adv. 6 (2016) 63991–64002, doi:\bibinfo{doi}{10.1039/C6RA12021K}.

[15] F. Koopman, N. Wierckx, J. H. de Winde, H. J. Ruijssenaars, Efficient whole-cell biotransformation of 5-(hydroxymethyl)furfural into FDCA, 2,5-furandicarboxylic acid, Bioresour. Technol. 101 (16) (2010) 6291 – 6296, ISSN 0960-8524, doi:\bibinfo{doi}{https://doi.org/10.1016/j.biortech.2010.03.050}.

[16] S. P. Teong, G. Yi, Y. Zhang, Hydroxymethylfurfural production from bioresources: past, present and future, Green Chem. 16 (2014) 2015–2026, doi:\bibinfo{doi}{10.1039/C3GC42018C}.

[17] X. Kong, Y. Zhu, Z. Fang, J. A. Kozinski, I. S. Butler, L. Xu, H. Song, X. Wei, Catalytic conversion of 5-hydroxymethylfurfural to some value-added derivatives, Green Chem. 20 (2018) 3657–3682, doi:\bibinfo{doi}{10.1039/C8GC00234G}.

[18] Z. Zhang, K. Deng, Recent Advances in the Catalytic Synthesis of 2,5-Furandicarboxylic Acid and Its Derivatives, ACS Catal. 5 (11) (2015) 6529–6544, doi:\bibinfo{doi}{10.1021/acscatal.5b01491}.

[19] A. Chatzidimitriou, J. Q. Bond, Oxidation of levulinic acid for the production of maleic anhydride: breathing new life into biochemicals, Green Chem. 17 (2015) 4367–4376, doi:\bibinfo{doi}{10.1039/C5GC01000D}.

[20] J. J. Bozell, L. Moens, D. Elliott, Y. Wang, G. Neuenscwander, S. Fitzpatrick, R. Bilski, J. Jarnefeld, Production of levulinic acid and use as a platform chemical for derived products, Resour., Conserv. and Recy. 28 (3) (2000) 227 – 239, ISSN 0921-3449, doi:\bibinfo{doi}{https://doi.org/10.1016/S0921-3449(99)00047-6}.

[21] K. Yan, C. Jarvis, J. Gu, Y. Yan, Production and catalytic transformation of levulinic acid: A platform for speciality chemicals and fuels, Renew. Sust. Energ. Rev. 51 (2015) 986 – 997, ISSN 1364-0321, doi:\bibinfo{doi}{https://doi.org/10.1016/j.rser.2015.07.021}.

[22] C. M. Cai, T. Zhang, R. Kumar, C. E. Wyman, Integrated furfural production as a renewable fuel and chemical platform from lignocellulosic biomass, J. Chem. Technol. Biotechnol. 89 (1) (2016) 2–10, doi:\bibinfo{doi}{10.1002/jctb.4168}.

[23] R. Mariscal, P. Maireles-Torres, M. Ojeda, I. Sdaba, M. Lpez Granados, Furfural: a renewable and versatile platform molecule for the synthesis of chemicals and fuels, Energy Environ. Sci. 9 (2016) 1144–1189, doi:\bibinfo{doi}{10.1039/C5EE02666K}.

[24] X. Li, P. Jia, T. Wang, Furfural: A Promising Platform Compound for Sustainable

552 Production of C4 and C5 Chemicals, ACS Catal. 6 (11) (2016) 7621–7640,
553 doi:\bibinfo{doi}{10.1021/acscatal.6b01838}.

554 [25] D. M. Alonso, S. G. Wettstein, J. A. Dumesic, Gamma-valerolactone, a sustainable
555 platform molecule derived from lignocellulosic biomass, Green Chem. 15 (2013)
556 584–595, doi:\bibinfo{doi}{10.1039/C3GC37065H}.

557 [26] J. Sherwood, M. De bruyn, A. Constantinou, L. Moity, C. R. McElroy, T. J. Farmer,
558 T. Duncan, W. Raverty, A. J. Hunt, J. H. Clark, Dihydrolevoglucosenone (Cyrene)
559 as a bio-based alternative for dipolar aprotic solvents, Chem. Commun. 50 (2014)
560 9650–9652, doi:\bibinfo{doi}{10.1039/C4CC04133J}.

561 [27] G. Wang, M. Jiang, Q. Zhang, R. Wang, G. Zhou, Biobased multiblock
562 copolymers: Synthesis, properties and shape memory performance of poly(ethylene
563 2,5-furandicarboxylate)-b-poly(ethylene glycol), Polym. Degrad. Stab. 144 (2017) 121
564 – 127, ISSN 0141-3910, doi:\bibinfo{doi}{https://doi.org/10.1016/j.polymdegradstab.
565 2017.07.032}.

566 [28] Y. Román-Leshkov, C. J. Barrett, Z. Y. Liu, J. A. Dumesic, Production of
567 dimethylfuran for liquid fuels from biomass-derived carbohydrates, Nature 447 (2007)
568 982 EP –.

569 [29] W. Yang, A. Sen, Direct Catalytic Synthesis of 5-Methylfurfural from
570 Biomass-Derived Carbohydrates, ChemSusChem 4 (3) (2011) 349–352,
571 doi:\bibinfo{doi}{10.1002/cssc.201000369}.

572 [30] B. Hu, Q. Lu, X. Jiang, X. Dong, M. Cui, C. Dong, Y. Yang, Pyrolysis mechanism
573 of glucose and mannose: The formation of 5-hydroxymethyl furfural and furfural, J.
574 Energ. Chem. 27 (2) (2018) 486 – 501, ISSN 2095-4956, doi:\bibinfo{doi}{https:
575 //doi.org/10.1016/j.jechem.2017.11.013}.

576 [31] B. n. Puértolas, Q. Imtiaz, C. R. Müller, J. Pérez-Ramírez, Platform Chemicals via

Zeolite-Catalyzed Fast Pyrolysis of Glucose, ChemCatChem 9 (9) (2017) 1579–1582, doi:\bibinfo{doi}{10.1002/cctc.201601052}.

[32] X. Chen, Y. Chen, Z. Chen, D. Zhu, H. Yang, P. Liu, T. Li, H. Chen, Catalytic fast pyrolysis of cellulose to produce furan compounds with SAPO type catalysts, J. Anal. Appl. Pyrolysis 129 (2018) 53 – 60, ISSN 0165-2370, doi:\bibinfo{doi}{https://doi.org/10.1016/j.jaap.2017.12.004}.

[33] L. Jiang, A. Zheng, Z. Zhao, F. He, H. Li, N. Wu, The comparison of obtaining fermentable sugars from cellulose by enzymatic hydrolysis and fast pyrolysis, Bioresour. Technol. 200 (2016) 8 – 13, ISSN 0960-8524, doi:\bibinfo{doi}{https://doi.org/10.1016/j.biortech.2015.09.096}.

[34] A. Zheng, T. Chen, J. Sun, L. Jiang, J. Wu, Z. Zhao, Z. Huang, K. Zhao, G. Wei, F. He, H. Li, Toward Fast Pyrolysis-Based Biorefinery: Selective Production of Platform Chemicals from Biomass by Organosolv Fractionation Coupled with Fast Pyrolysis, ACS Sustain. Chem. Eng. 5 (8) (2017) 6507–6516, doi:\bibinfo{doi}{10.1021/acssuschemeng.7b00622}.

[35] M. Carrier, M. Windt, B. Ziegler, J. Appelt, B. Saake, D. Meier, A. Bridgwater, Quantitative Insights into the Fast Pyrolysis of Extracted Cellulose, Hemicelluloses, and Lignin, ChemSusChem 10 (16) (2017) 3212–3224, doi:\bibinfo{doi}{10.1002/cssc.201700984}.

[36] R. Garrido, J. Reckamp, J. Satrio, Effects of Pretreatments on Yields, Selectivity and Properties of Products from Pyrolysis of Phragmites australis (Common Reeds), Environments 4 (2017) 1–13, doi:\bibinfo{doi}{10.3390/environments4040096}.

[37] L. Luque, R. Westerhof, G. V. Rossum, S. Oudenhoven, S. Kersten, F. Berruti, L. Rehmann, Pyrolysis based bio-refinery for the production of bioethanol from demineralized ligno-cellulosic biomass, Bioresour. Technol. 161 (2014) 20 – 28, ISSN 0960-8524, doi:\bibinfo{doi}{https://doi.org/10.1016/j.biortech.2014.03.009}.

[38] C. Di Blasi, C. Branca, A. Galgano, Biomass Screening for the Production of Furfural via Thermal Decomposition, Ind. Eng. Chem. Res. 49 (6) (2010) 2658–2671, doi:\bibinfo{doi}{10.1021/ie901731u}.

[39] V. Savou, G. Grause, S. Kumagai, Y. Saito, T. Kameda, T. Yoshioka, Pyrolysis of sugarcane bagasse pretreated with sulfuric acid, J. Energy Inst. ISSN 1743-9671, doi:\bibinfo{doi}{https://doi.org/10.1016/j.joei.2018.06.003}.

[40] T. Mani, P. Murugan, N. Mahinpey, Pyrolysis of Oat Straw and the Comparison of the Product Yield to Wheat and Flax Straw Pyrolysis, Energy Fuels 25 (7) (2011) 2803–2807, doi:\bibinfo{doi}{10.1021/ef200546v}.

[41] D. Cooper, On the Structure of the Nut Know as Vegetable Ivory, Transactions of The Microscopical Society & Journal 1 (1) (1842) 97–99, doi:\bibinfo{doi}{10.1111/j.1365-2818.1842.tb06276.x}.

[42] F. M. Oña Caiza, Estudio del efecto de la incorporación de partículas provenientes de los residuos de tagua (*Phytelephas aequatorialis macrocarpa*) a una matriz de poliestireno, http://bibdigital.epn.edu.ec/handle/15000/17024, 2017.

[43] T. E. Timell, Vegetable ivory as a source of mannan polysaccharide, Canadian J. Chem. 35 (4) (1957) 333–338, doi:\bibinfo{doi}{10.1139/v57-048}.

[44] J. Patterson, CXXIX.Investigation of the mannan present in vegetable ivory, J. Chem. Soc., Trans. 123 (1923) 1139–1149, doi:\bibinfo{doi}{10.1039/CT9232301139}.

[45] G. O. Aspinall, E. L. Hirst, E. G. V. Percival, I. R. Williamson, The mannans of ivory nut (Phytelephas macrocarpa). Part I. The methylation of mannan A and mannan B, J. Chem. Soc. (1953) 3184–3188doi:\bibinfo{doi}{10.1039/JR9530003184}.

[46] R. H. Furneaux, F. Shafizadeh, Pyrolytic production of 1,6-anhydro-β-D-mannopyranose, Carbohyr. Res. 74 (1) (1979) 354 – 360, ISSN 0008-6215, doi:\bibinfo{doi}{https://doi.org/10.1016/S0008-6215(00)84794-1}.

[47] A. E. Knauf, R. M. Hann, C. S. Hudson, D-Mannosan¡1,5¿β¡1,6¿ or Levomannosan, J. Am. Chem. Soc. 63 (5) (1941) 1447–1451, doi:\bibinfo{doi}{10.1021/ja01850a088}.

[48] T. Zhang, Z. Pan, C. Qian, X. Chen, Isolation and purification of D-mannose from palm kernel, Carbohyr. Res. 344 (13) (2009) 1687 – 1689, ISSN 0008-6215, doi:\bibinfo{doi}{https://doi.org/10.1016/j.carres.2009.06.018}.

[49] Y. Chu, M. A. Meyers A, B. Wang, W. Yang, J.-Y. Jung, C. F. M. Coimbra, A Sustainable Substitute for Ivory: the Jarina Seed from the Amazon, Sci. Rep. 5 (2015) 14387 EP –, article.

[50] A. S. Barfod, B. Bergmann, H. B. Pedersen, The Vegetable Ivory Industry: Surviving and Doing Well in Ecuador, Economic Botany 44 (3) (1990) 293–300, ISSN 00130001, 18749364.

[51] C. S. Hudson, H. L. Sawyer, The preparation of pure chrystalline mannose and a study of its mutarotation, J. Am. Chem. Soc. 39 (3) (1917) 470–478, doi:\bibinfo{doi}{10.1021/ja02248a016}.

[52] C. S. Hudson, E. L. Jackson, Improvements in the Preparation of Crystalline D-Mannose, J. Am. Chem. Soc. 56 (4) (1934) 958–959, doi:\bibinfo{doi}{10.1021/ja01319a063}.

[53] A. Enders, J. Lehmann, Proximate analyses for characterizing biochars, chap. 2, CSIRO Publishing, ISBN ISBN 9781498765534 - CAT# K29083, 9–22, 2017.

[54] ASTM D1762-84, Standard Test Method for Chemical Analysis of Wood Charcoal, Standard, ASTM International, West Conshohocken, PA, doi:\bibinfo{doi}{DOI:10.1520/D1762}, 2013.

[55] G. Yildiz, M. Pronk, M. Djokic, K. M. van Geem, F. Ronsse, R. van Duren, W. Prins, Validation of a new set-up for continuous catalytic fast pyrolysis of biomass coupled with vapour phase upgrading, J. Anal. Appl. Pyrolysis 103 (2013) 343 – 351, ISSN 0165-2370, doi:\bibinfo{doi}{https://doi.org/10.1016/j.jaap.2013.02.001}.

[56] C. Mohabeer, L. Abdelouahed, S. Marcotte, B. Taouk, Comparative analysis of pyrolytic liquid products of beech wood, flax shives and woody biomass components, J. Anal. Appl. Pyrolysis 127 (2017) 269 – 277, ISSN 0165-2370, doi:\bibinfo{doi}{https://doi.org/10.1016/j.jaap.2017.07.025}.

[57] S. Channiwala, P. Parikh, A unified correlation for estimating HHV of solid, liquid and gaseous fuels, Fuel 81 (8) (2002) 1051 – 1063, ISSN 0016-2361, doi:\bibinfo{doi}{https://doi.org/10.1016/S0016-2361(01)00131-4}.

[58] C. Sheng, J. Azevedo, Estimating the higher heating value of biomass fuels from basic analysis data, Biomass Bioenergy 28 (5) (2005) 499 – 507, ISSN 0961-9534, doi:\bibinfo{doi}{https://doi.org/10.1016/j.biombioe.2004.11.008}.

[59] A. Enders, S. Sohi, J. Lehmann, B. Singh, Total elements analysis of metals and nutrients in biochars, chap. 9, CSIRO Publishing, ISBN ISBN 9781498765534 - CAT# K29083, 95–108, 2017.

[60] A. Cross, S. P. Sohi, A method for screening the relative long-term stability of biochar, GCB Bioenerg. 5 (2) (2013) 215–220, doi:\bibinfo{doi}{10.1111/gcbb.12035}.

[61] H. Yang, R. Yan, H. Chen, D. H. Lee, C. Zheng, Characteristics of hemicellulose, cellulose and lignin pyrolysis, Fuel 86 (12) (2007) 1781 – 1788, ISSN 0016-2361, doi:\bibinfo{doi}{https://doi.org/10.1016/j.fuel.2006.12.013}.

[62] R. Venderbosch, W. Prins, Fast pyrolysis technology development, Biofuel. Bioprod. Biorefin. 4 (2) (2010) 178–208, doi:\bibinfo{doi}{10.1002/bbb.205}.

[63] M. J. Kozioł, H. B. Pedersen, Phytelephas aequatorialis (Arecaceae) in Human and Animal Nutrition, Economic Botany 47 (4) (1993) 401–407, ISSN 00130001, 18749364.

[64] D. L. Dalluge, T. Daugaard, P. Johnston, N. Kuzhiyil, M. M. Wright, R. C. Brown, Continuous production of sugars from pyrolysis of acid-infused lignocellulosic

biomass, Green Chem. 16 (2014) 4144–4155, doi:\bibinfo{doi}{10.1039/C4GC00602J}.

[65] L. Luque, S. Oudenhoven, R. Westerhof, G. van Rossum, F. Berruti, S. Kersten, L. Rehmann, Comparison of ethanol production from corn cobs and switchgrass following a pyrolysis-based biorefinery approach, Biotechnology for Biofuels 9 (1) (2016) 242, ISSN 1754-6834, doi:\bibinfo{doi}{10.1186/s13068-016-0661-4}.

[66] P. Marathe, S. Oudenhoven, P. Heerspink, S. Kersten, R. Westerhof, Fast pyrolysis of cellulose in vacuum: The effect of potassium salts on the primary reactions, Chem. Eng. J. 329 (2017) 187 – 197, ISSN 1385-8947, doi:\bibinfo{doi}{https://doi.org/10.1016/j.cej.2017.05.134}, xXII International conference on Chemical Reactors CHEMREACTOR-22.

[67] P. R. Patwardhan, D. L. Dalluge, B. H. Shanks, R. C. Brown, Distinguishing primary and secondary reactions of cellulose pyrolysis, Bioresour. Technol. 102 (8) (2011) 5265 – 5269, ISSN 0960-8524, doi:\bibinfo{doi}{https://doi.org/10.1016/j.biortech.2011.02.018}.

[68] P. R. Patwardhan, R. C. Brown, B. H. Shanks, Product Distribution from the Fast Pyrolysis of Hemicellulose, ChemSusChem 4 (5) (2011) 636–643, doi:\bibinfo{doi}{10.1002/cssc.201000425}.

[69] G. Bonneau, A. A. M. Peru, A. L. Flourat, F. Allais, Organic solvent- and catalyst-free BaeyerVilliger oxidation of levoglucosenone and dihydrolevoglucosenone (Cyrene): a sustainable route to (S)-γ-hydroxymethyl-α,β-butenolide and (S)-γ-hydroxymethyl-γ-butyrolactone, Green Chem. 20 (2018) 2455–2458, doi:\bibinfo{doi}{10.1039/C8GC00553B}.

[70] T. Vijai Kumar Reddy, G. Sandhya Rani, R. B. N. Prasad, B. L. A. Prabhavathi Devi, Green recyclable SO3H-carbon catalyst for the selective synthesis of

isomannide-based fatty acid monoesters as non-ionic bio-surfactants, RSC Adv. 5 (2015) 40997–41005, doi:\bibinfo{doi}{10.1039/C5RA03605D}.

[71] S. Jia, X. He, Z. Xu, Valorization of an underused sugar derived from hemicellulose: efficient synthesis of 5-hydroxymethylfurfural from mannose with aluminum salt catalyst in dimethyl sulfoxide/water mixed solvent, RSC Adv. 7 (2017) 39221–39227, doi:\bibinfo{doi}{10.1039/C7RA07803J}.

[72] S. H. Krishna, T. W. Walker, J. A. Dumesic, G. W. Huber, Kinetics of Levoglucosenone Isomerization, ChemSusChem 10 (1) (2016) 129–138, doi:\bibinfo{doi}{10.1002/cssc.201601308}.

[73] Crombie, Kyle and Mašek, Ondřej, Pyrolysis biochar systems, balance between bioenergy and carbon sequestration, GCB Bioenerg. 7 (2) (2015) 349–361, ISSN 1757-1707, doi:\bibinfo{doi}{10.1111/gcbb.12137}.

[74] J. Lehmann, J. Gaunt, M. Rondon, Bio-char Sequestration in Terrestrial Ecosystems – A Review, Mitig. Adapt. Strat. Global Change 11 (2) (2006) 403–427, ISSN 1573-1596, doi:\bibinfo{doi}{10.1007/s11027-005-9006-5}.

[75] S. Ghysels, M. S. I. Mozumder, H. D. Wever, E. I. Volcke, L. Garcia-Gonzalez, Targeted poly(3-hydroxybutyrate-co-3-hydroxyvalerate) bioplastic production from carbon dioxide, Bioresour. Technol. 249 (2018) 858 – 868, ISSN 0960-8524, doi:\bibinfo{doi}{https://doi.org/10.1016/j.biortech.2017.10.081}.

[76] Y. Fan, D. Zhang, A. Zheng, Z. Zhao, H. Li, T. Yang, Selective production of anhydrosugars and furfural from fast pyrolysis of corncobs using sulfuric acid as an inhibitor and catalyst, Chem. Eng. J. 358 (2019) 743 – 751, ISSN 1385-8947, doi:\bibinfo{doi}{https://doi.org/10.1016/j.cej.2018.10.014}.

[77] P. P. Upare, J.-W. Yoon, M. Y. Kim, H.-Y. Kang, D. W. Hwang, Y. K. Hwang, H. H. Kung, J.-S. Chang, Chemical conversion of biomass-derived hexose sugars to levulinic

729 acid over sulfonic acid-functionalized graphene oxide catalysts, Green Chem. 15
730 (2013) 2935–2943, doi:\bibinfo{doi}{10.1039/C3GC40353J}.

731 [78] X. Li, Y. Zhang, The conversion of 5-hydroxymethyl furfural (HMF) to maleic
732 anhydride with vanadium-based heterogeneous catalysts, Green Chem. 18 (2016)
733 643–647, doi:\bibinfo{doi}{10.1039/C5GC01794G}.

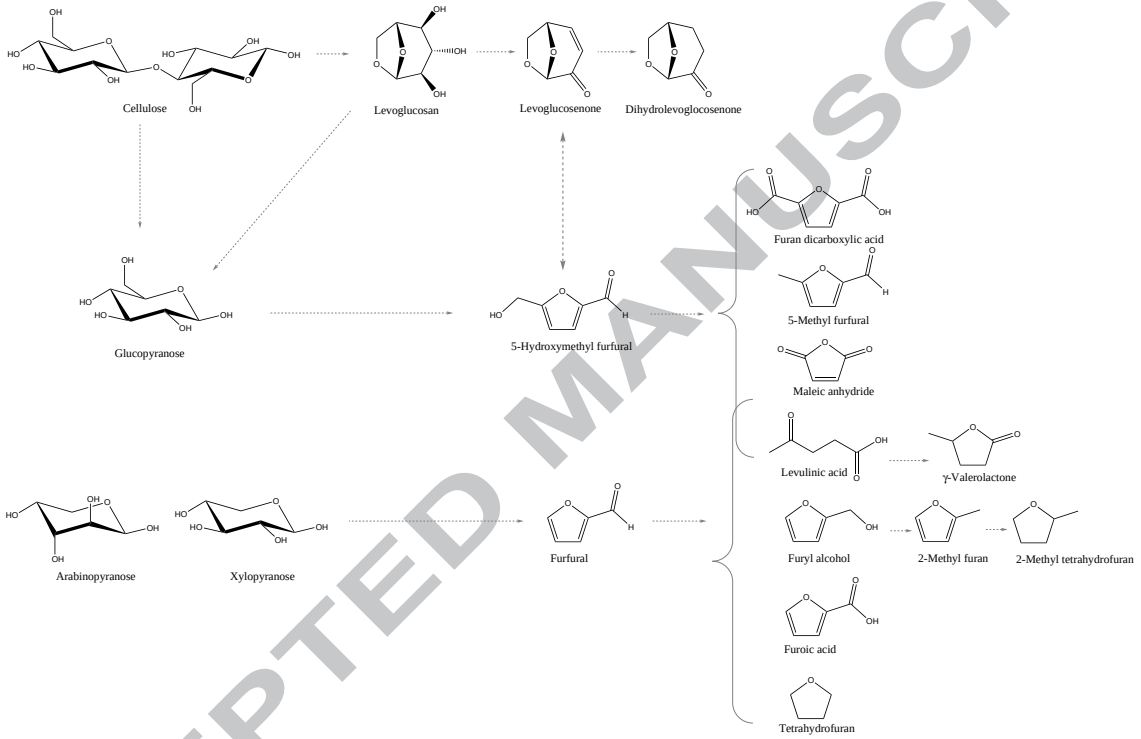

Figure 1: Selection of some key carbohydrate-derived platform chemicals and products. Scheme compiled from Takkellapati et al. [7], Farmer and Mascal [1], Krishna et al. [72], Upare et al. [77], Chatzidimitriou and Bond [19], Li and Zhang [78], Sherwood et al. [26].

Figure 2: Top row: *Phytelephas aequatorialis* palm and its fruit, i.e. ivory nut. Bottom row: crafted products and cutting residues used within this study.

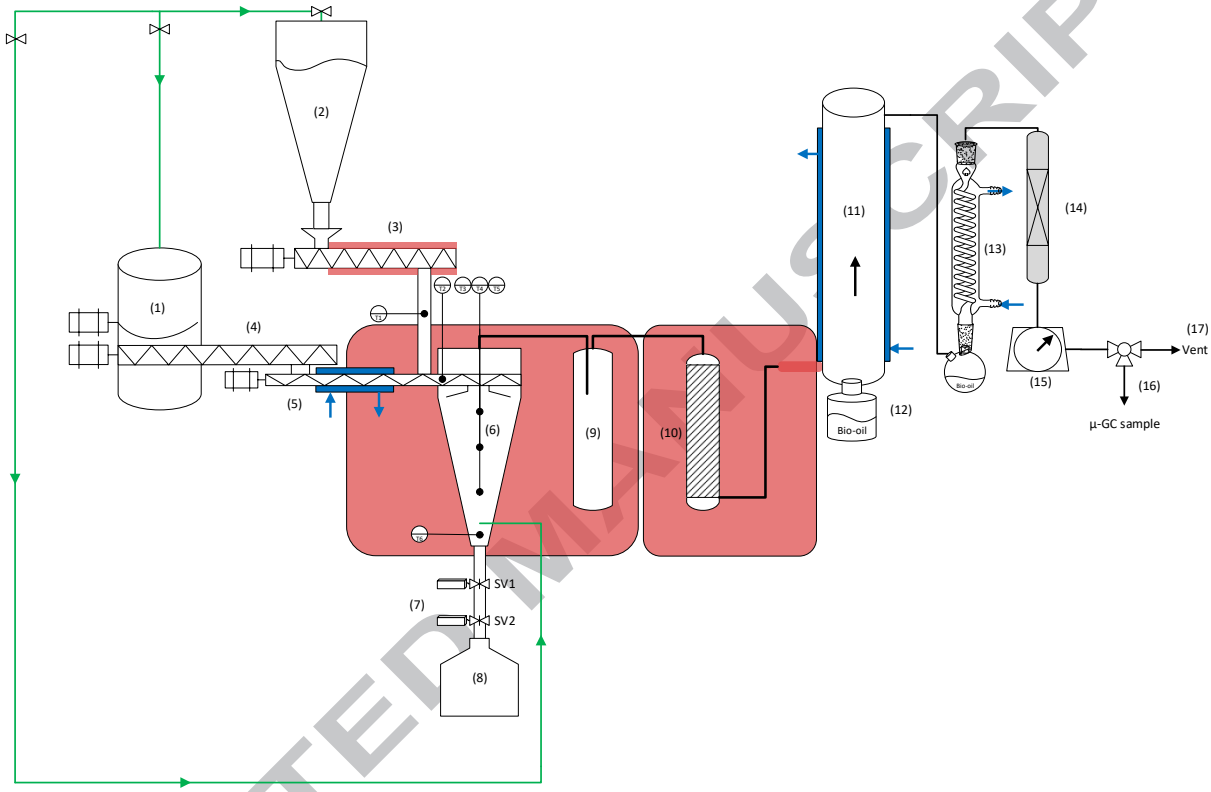

Figure 3: Scheme of the fully equipped lab-scale reactor. (1) biomass hopper; (2) sand hopper; (3) sand conveyor; (4) biomass conveyor; (5) reactor conveyor or auger screw with cooling jacket; (6) *in-situ* reactor; (7) pistons; (8) solid collection vessel; (9) knock-out vessel; (10) second knock-out vessel; (11) electrostatic precipitator); (12) liquid collection vessel; (13) glass condenser; (14) cotton wool filter; (15) gas meter; (16) exhaust system; (17) micro-GC sample line.

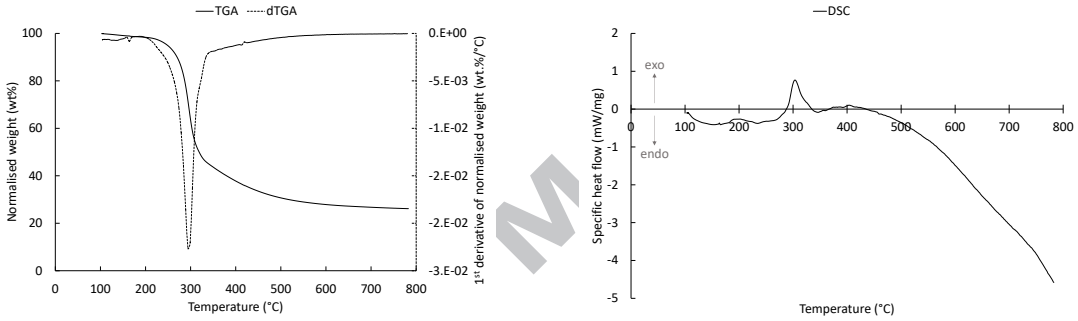

(a) (b)

Figure 4: Results for (a) the thermogravimetric analysis and weight-loss rate of ivory nut, (b) differential scanning calorimetry of ivory nut.

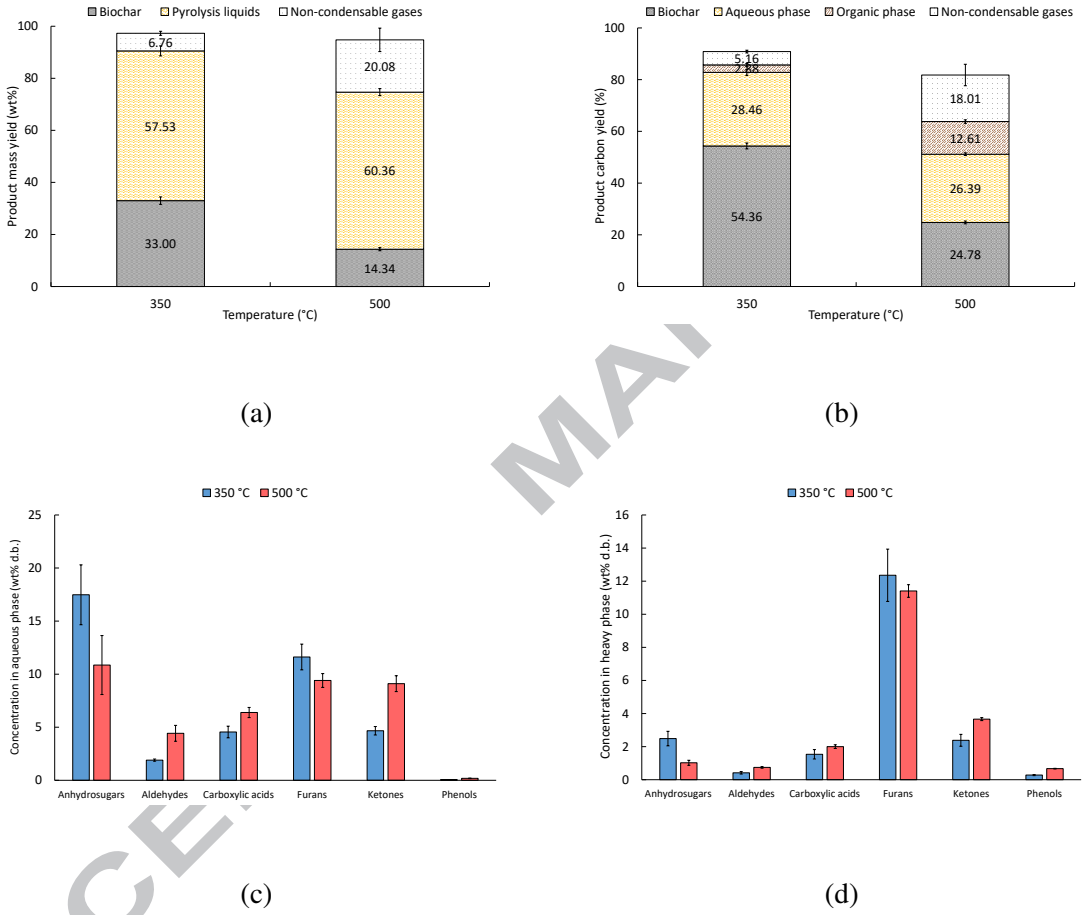

Figure 5: Results for (a) product yield after pyrolysis, (b) carbon distribution within pyrolysis products, (c) composition of aqueous phase and (d) composition of organic phase.

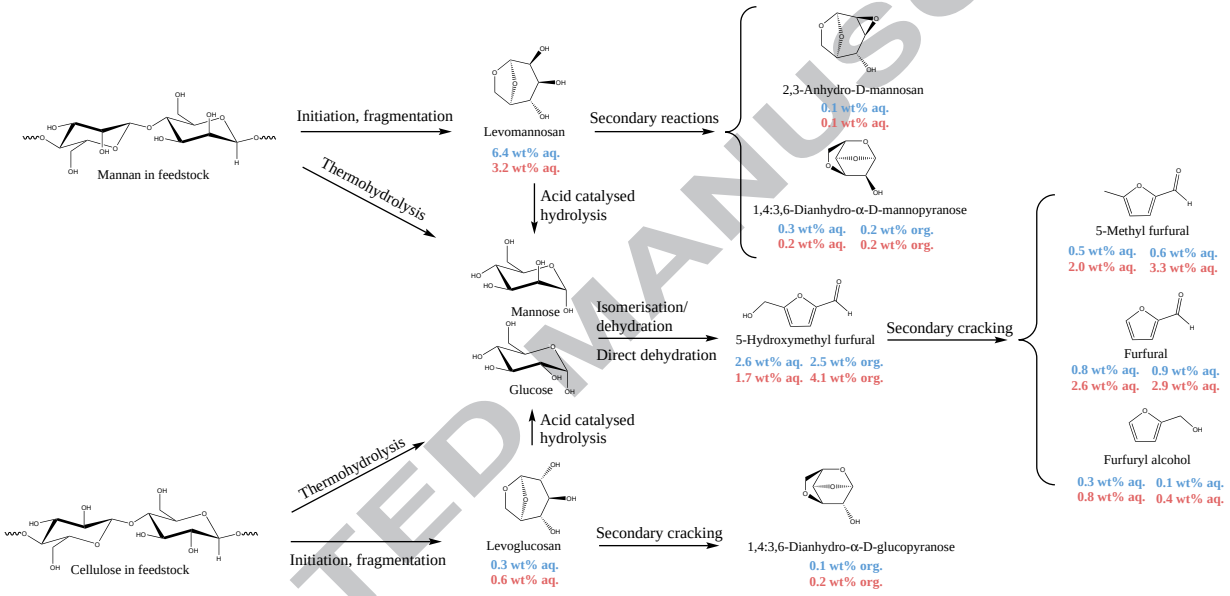

Figure 6: Possible pyrolysis pathways in fast pyrolysis of ivory nut. Significant yields are indicated on pyrolysis liquid basis (as produced). Blue: yield after pyrolysis at 350 °C, red: yield after pyrolysis at 500 °C.

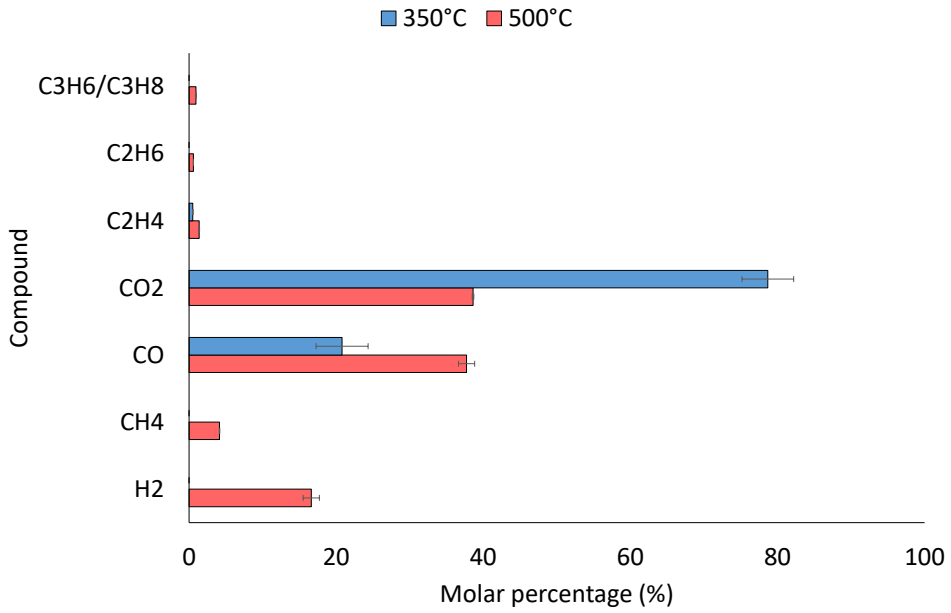

Figure 7: Composition of non-condensable gases evolved during pyrolysis at 350 °C and 500 °C of vegetable ivory.

Table 1: Comparison of evolved compounds during micropyrolysis (Py–GC/MS) of ivory nut and cellulose. The evolved compounds from ivory nut, which had a TIC area% larger than 1% are reported and compared to the TIC area% of cellulose. RT: GC retention time. TIC area% presents the component peak area divided by the total peak area.

	Ivory nut		Cellulose	
Compound	RT (min)	TIC area %	RT (min)	TIC area %
Levomannosan	40.68	53.00	40.62	0.43
5-HMF	33.41	5.71	33.42	0.72
Hydroxy-acetaldehyde	7.58	4.23	7.58	3.29
1-Hydroxy-2-propanone	10.04	2.89	10.05	0.46
Furfural	15.92	2.68	15.94	0.71
Levoglucosan	42.36	2.25	42.54	75.25
2-Furanmethanol	17.44	2.08	17.48	0.08
Acetic acid	8.77	1.84	8.79	0.10
2-Oxo-propanoic acid methyl ester	15.39	1.55	15.40	0.42
3,5-Dihydroxy-2-methyl-4H-Pyran-4-one	28.41	1.42	28.43	0.11
5-Methyl-2-furancarboxaldehyde	20.87	1.11	20.87	0.18

Table 2: Elemental composition of the pyrolysis liquids on an as-produced basis (a.p.) and on a dry basis (d.b.). [a]Assumed equal to the water content from the organic phase of 500 °C.

	350 °C		500 °C	
wt%	a.p.	d.b.	a.p.	d.b.
N-org.	1.07 ± 0.64	1.22 ± 0.73	1.93 ± 0.08	2.20 ± 0.10
C-org.	54.68 ± 1.00	62.42 ± 1.20	60.01 ± 0.76	68.51 ± 0.95
H-org.	6.50 ± 0.38	5.86 ± 0.43	7.38 ± 0.07	6.87 ± 0.09
O-org.	37.76 ± 1.73	41.55 ± 1.99	30.68 ± 0.75	33.47 ± 0.88
N-aq.	0.63 ± 0.03	1.56 ± 0.10	0.93 ± 0.02	2.30 ± 0.15
C-aq.	19.91 ± 0.33	49.47 ± 2.54	19.82 ± 0.81	49.25 ± 3.59
H-aq.	9.70 ± 0.07	7.77 ± 1.18	9.95 ± 0.10	8.39 ± 1.48
O-aq.	69.76 ± 0.36	41.21 ± 8.46	69.30 ± 0.80	40.06 ± 10.36

	350 °C		500 °C	
Water content (%)	Aqueous phase	Organic phase	Aqueous phase	Organic phase
	59.75 ± 1.95	12.41 ± 0.49[a]	61.55 ± 2.17	12.41 ± 0.49

Pyrolytic water	350 °C	500 °C
yield (wt.%)	23.95 ± 0.23	23.69 ± 2.64

Table 3: Proximate and elemental analysis of biochar obtained upon pyrolysis at 350 °C and 500 °C. VM: volatile matter; Ash: ash content; FC: fixed carbon content; d.b.: dry basis; d.a.f.: dry and ash-free basis; H/C and O/C are molar ratios.

	Proximate analysis (wt% d.b.)					Ultimate analysis (wt% d.b.)						Carbon stability
Pyrolysis temperature	Biochar yield	VM	Ash	FC	FC yield	N	C	H	O	H/C	O/C	(%)
350	36.87	41.16	3.31	53.40	19.87	1.38	65.48	4.18	25.65	0.77	0.29	40.57
	±1.41	±0.23	±0.05	±0.63	±0.48	±0.07	±1.19	±0.12	±1.12	±0.03	±0.02	±1.83
500	15.82	20.36	7.73	68.56	10.96	1.43	69.59	2.93	18.31	0.51	0.20	64.56
	±0.73	±0.57	±0.82	±1.51	±0.80	±0.06	±2.20	±0.07	±2.57	±0.02	±0.04	±1.77

Table 4: Ash composition of the feedstock and biochar obtained after pyrolysis at 350 °C and 500 °C.

Element	Unit	Ivory nut	Biochar 350 °C	Biochar 500 °C
Ca	$g.kg^{-1}$	0.43	1.86	5.49
Mg	$g.kg^{-1}$	0.25	2.03	2.64
K	$g.kg^{-1}$	1.25	11.97	8.22
Na	$g.kg^{-1}$	0.33	0.56	0.80
Cr	$mg.kg^{-1}$	0.71	26.23	22.73
Mn	$mg.kg^{-1}$	6.04	32.15	46.53
Fe	$g.kg^{-1}$	0.01	0.19	0.18
Co	$mg.kg^{-1}$	0.03	0.67	0.17
Ni	$mg.kg^{-1}$	0.93	22.04	19.09
Cu	$mg.kg^{-1}$	7.59	31.23	60.29
Zn	$mg.kg^{-1}$	10.81	45.66	79.46

Table 5: Higher heating value (HHV, MJ.kg^{-1}) on dry basis of the feedstock, and produced biochar (measured) and the pyrolysis liquid phases (calculated) on dry and as-received basis, along with the water content of the pyrolysis liquid phases. [a]Measured through bomb calorimetry. [b]Calculated through Eq. 4-5.

	Pyrolysis temperature (°C)	HHV (MJ/kg)
Feedstock	/	21.12 ± 2.17
Biochar[a]	350	27.12 ± 0.37
	500	28.37 ± 0.76
Pyr. liq. (aq.)[b]	350	21.89
	500	22.55
pyr. liq. (organic)[b]	350	24.19
	500	28.19

GHENT UNIVERSITY
FACULTY OF BIOSCIENCE ENGINEERING

Highlights

Subject: Submission in *Chemical Engineering Journal* Special Issue: "Thermochemical Conversion of Biowaste on Energy and Resource Recovery and Pollution Abatement".

Dear Editor and Referees,

Kindly find enclosed our highlights for the manuscript entitled "*Fast pyrolysis of mannan-rich ivory nut (Phytelephas aequatorialis) to valuable biorefinery products".*

- Fast pyrolysis of mannan-rich ivory nut was performed at 350°C and 500°C
- Pyrolysis liquids (yield 58-60 wt%) were rich in levomannosan and 5-hydroxymethyl furfural
- Biochar and non-condensible gases (NCGs) were characterized
- Biochar holds potential for e.g. soil applications, NCGs hold potential for e.g. syngas processes

Yours sincerely,

Stef Ghysels (on behalf of all authors)

DEPARTMENT – GREEN CHEMISTRY & TECHNOLOGY
RESEARCH GROUP – THERMOCHEMICAL CONVERSION OF BIOMASS